

## Low-energy electron elastic collision cross sections for ground and excited Tm, Lu and Hf atoms

Z. Felfli<sup>a,\*</sup>, A.Z. Msezane<sup>a</sup>, D. Sokolovski<sup>b,c</sup>

<sup>a</sup> Department of Physics and Centre for Theoretical Studies of Physical Systems, Clark Atlanta University, Atlanta, GA 30314, USA

<sup>b</sup> School of Mathematics and Physics, Queen's University of Belfast, Belfast, BT7 1NN, UK

<sup>c</sup> Department of Chemical Physics, University of the Basque Country, Leioa, Spain

### ARTICLE INFO

#### Article history:

Received 2 September 2010

Received in revised form 27 January 2011

Available online 4 March 2011

#### Keywords:

Elastic scattering  
Chemical reactions  
Resonances  
Regge poles  
Catalysis  
Electron affinity  
Negative ions

### ABSTRACT

Low-energy  $0 \leq E \leq 1.0$  eV electron elastic scattering from ground and excited Tm, Lu and Hf atoms has been investigated. Both total and differential cross sections have been calculated; the latter at the scattering angles  $\theta = 0^\circ, 90^\circ$  and  $180^\circ$ . The recent Regge-pole methodology has been used for the calculations. In the method the crucial electron–electron correlation effects are accounted for through the Mulholland formula. We find that the total cross sections are characterized generally by shape resonances, Ramsauer-Townsend minima and dramatically sharp long-lived resonances from which we extract the binding energies of the negative ions. Our extracted binding energy of the  $\text{Hf}^-$  negative ion from the total cross section is compared with that of Pan and Beck [14].

© 2011 Elsevier B.V. All rights reserved.

### 1. Introduction

Recently, we explored the near-threshold electron–atom scattering through the calculation of the elastic total cross sections (TCSs) for Au and Pd [1]. The objective was to understand at the fundamental atomic level the observed excellent catalytic properties of Au and Pd nanoparticles and the exceptional catalytic activity of the Au–Pd catalyst when catalyzing  $\text{H}_2\text{O}_2$  [2,3]. How Pd and Au–Pd promote catalysis exactly remains a subject of considerable academic and industrial interest [4]. We proposed the interplay between the negative ion resonances and Ramsauer-Townsend minima that characterize the electron elastic TCSs as the fundamental mechanism underlying nanoparticle catalysis [1]. Thus, there is a need for the identification and delineation of the resonance structures and minima in the electron collision TCSs for atoms in the near threshold energy region.

Inter-shell-type resonances result when an electron attaches itself to a neutral atom with the formation of a very weakly bound negative ion [5]. A negative ion may be considered as the bound-state limit of the electron–neutral atomic system. The understanding of chemical reactions involving negative ions requires accurate binding energies (BEs). Generally, strong scattering resonances characterize electron interactions at low energies. They involve

the temporary trapping of the projectile in the field of the atom or molecule. These resonances often impact significantly the scattering cross sections and, in some cases, they can enhance scattering rates by orders of magnitude [6].

Due to their low BEs bound single excited states are very rare in negative ions [7]. Perhaps, this is why it has been over a decade since infrared laser spectroscopy [8] was employed to accurately measure the BEs of the bound excited  $np^3 \ ^2D$  terms of the  $\text{Si}^-$ ,  $\text{Ge}^-$  and  $\text{Sn}^-$  negative ions. The term averaged BEs for the ground states of the  $\text{Sn}^-$  and  $\text{Ge}^-$  anions were also determined [9] as well as for the  $\text{Si}^-$  anion [10]. A bound excited state of the  $\text{La}^-$  negative ion was observed using laser photoelectron energy spectroscopy [11] and its BE relative to the La ground state was measured. These very few available measurements on excited atomic negative ions have been vital to the benchmarking of the recent Regge pole methodology [12] in the context of calculating electron elastic cross sections for excited atoms, from which their BEs are extracted. Recently, the experimental BE of a metastable state of  $\text{Pt}^-$  [13] and the theoretical EA of Hf [14] have been reported.

Negative ions are weakly bound quantum systems with the outermost electron moving under the influence of a short-range core-polarization interaction. This contrasts with the infinite spectrum of bound states associated with the long-range Coulomb potential experienced by the outermost electron in an atom. In negative ions the core-polarization potential typically supports only a single bound state [15]. Various theoretical investigations have

\* Corresponding author. Tel.: +1 4048806970; fax: +1 4048808360.  
E-mail address: [zfelfli@cau.edu](mailto:zfelfli@cau.edu) (Z. Felfli).

demonstrated through comparisons with measurements the vital importance of the core–polarization interaction in low energy electron scattering from atoms and molecules [16–22]. Significantly, the calculated EA value for the Ba atom using a 23-state fully relativistic R-matrix calculation that neglected the core–polarization interaction [18] disagreed by a factor of about two with the measured value [20]. Over the years negative ions have attracted significant experimental investigations using various experimental techniques and for various reasons [23–27] and references therein. Recently, dramatically sharp long-lived resonances, characterizing the scattering of electrons from simple and complex atoms, have been identified. These have been interpreted as the signatures of the stable bound states of the relevant negative ions formed during the elastic collisions between the projectile and the target neutral atom [28,29].

The mechanism through which low-energy electron scattering deposits energy and induces chemical transitions is attributed to the formation of temporary negative ionic states and their properties [30]. The Wigner threshold law [31], shape resonances and Ramsauer-Townsend (R-T) minima generally characterize the near-threshold elastic scattering TCSs of electrons by neutral atoms. The Wigner threshold law is essential in high precision measurements of BEs of valence electrons using photodetachment threshold spectroscopy [32]. Shape resonances are useful for interpreting electron-induced chemical processes resulting in negative ion production [30]. The R-T minima, manifesting the polarization of the atomic core by the scattered electron [33], are important in understanding sympathetic cooling and the production of cold molecules from natural fermions [34].

In this paper we explore, following the recent success [1,35], low-energy  $E \leq 1.0$  eV elastic collisions between an electron and the complex atoms Tm, Lu and Hf through the calculation of the elastic TCSs and differential cross sections (DCSs) and search for long-lived resonances. These if they exist are manifestations of the formation of stable weakly bound ground and excited negative ions. From the energy positions of the characteristic resonances we extract the BEs of the excited negative ions.

## 2. Computational method

Understanding the structure and the dynamics of low-energy electron elastic collisions, resulting in the formation of negative ions as resonances, is quite challenging for conventional theoretical methods. These theoretical methods encounter difficulties because intricate and subtle interactions among the many diverse electron configurations generally characterize heavy and complex atoms. Calculating binding energies of excited anions is particularly more exacting because excited states are generally weakly bound, BEs <1 eV, but mostly tenuously bound, BEs <0.1 eV. It is in this context that the recent complex angular momentum (CAM) or Regge-pole methodology [12,36] has been developed; it calculates independently of measurements the elastic TCSs using the Mulholland formula [37]. This formula converts the infinite discrete sum into a background integral plus the contribution from a few poles to the process under consideration. The Regge-pole methodology requires no *a priori* knowledge of the experimental or other theoretical data as inputs.

Electron–electron correlations and core–polarization interactions are crucial for the existence and stability of most negative ions. The former effects are embedded in the Mulholland formula [12,36] for the TCS, while the latter interactions are incorporated through the well-investigated Thomas–Fermi (T-F) [38] type model potential [39,40]. Within the complex angular momentum,  $L$  description of scattering,  $\text{Im } L$  is used to distinguish between the shape resonances (short-lived resonances) and the stable bound

states of the negative ions (long-lived resonances) formed as Regge resonances in the electron–atom collision. For the latter the  $\text{Im } L$  is several orders-of-magnitude smaller than that for the former. The Mulholland formula [37] used here is of the form [12,36] (atomic units are used throughout):

$$\sigma_{\text{tot}}(E) = 4\pi k^{-2} \int_0^\infty \text{Re}[1 - S(\lambda)] \lambda d\lambda - 8\pi^2 k^{-2} \sum_n \text{Im} \frac{\lambda_n \rho_n}{1 + \exp(-2\pi i \lambda_n)} + I(E) \quad (1)$$

where  $\sigma_{\text{tot}}(E)$  is the TCS at impact energy  $E$ ,  $S$  is the  $S$ -matrix,  $k = \sqrt{2mE}$ , with  $m$  being the mass,  $\rho_n$  is the residue of the  $S$ -matrix at the  $n$ th pole,  $\lambda_n$  and  $I(E)$  contains the contributions from the integrals along the imaginary  $\lambda$ -axis; its contribution has been demonstrated to be negligible [29]. Note that  $\lambda$  is related to the complex angular momentum  $L$  through  $\lambda = L + 1/2$ . We will consider the case for which  $\text{Im } \lambda_n \ll 1$  so that for constructive addition,  $\text{Re } \lambda_n \approx 1/2, 3/2, 5/2, \dots$ , yielding  $\ell \equiv \text{Re } L \approx 0, 1, 2, \dots$ . The importance of Eq. (1) is that a resonance is likely to affect the elastic TCS when its Regge pole position is close to a real integer [12]. We also calculate the DCS from

$$d\sigma(E, \theta)/d\Omega = |f(E, \theta)|^2 \quad (2)$$

where  $d\sigma(E, \theta)/d\Omega$  is the differential cross section and the scattering amplitude  $f(E, \theta)$  can be expressed as a partial wave sum

$$f(E, \theta) = (1/2ik) \sum_{\ell=0}^{\infty} (2\ell + 1) P_\ell(\cos \theta) [S_\ell(E) - 1] \quad (3)$$

with  $k, \ell, \theta, P_\ell(\cos \theta)$  and  $S_\ell(E)$  being the wave vector, the angular momentum quantum number, the scattering angle, a Legendre polynomial of degree  $\ell$  and the scattering matrix element, respectively. For central field scattering

$$S_\ell(E) = \exp[i\delta(E, \ell)] \quad (4)$$

where  $\delta(E, \ell)$  are the phase shifts. For the calculation of both the TCSs and the DCSs the T-F type potential [38] takes the well investigated [39,40] form

$$U(r) = \frac{-Z}{r(1 + aZ^{1/3}r)(1 + bZ^{2/3}r^2)}, \quad (5)$$

where  $Z$  is the nuclear charge and  $a$  and  $b$  are adjustable parameters. For small  $r$ , the potential describes the Coulomb attraction between an electron and a nucleus,  $U(r) \sim -Z/r$ , while at large distances it mimics the polarization potential,  $U(r) \sim -1/(abr^4)$  and accounts properly for the vital core–polarization interaction at very low energies. The effective potential

$$V(r) = U(r) + L(L + 1)/(2r^2), \quad (6)$$

is considered here as a continuous function of the variables  $r$  and  $L$  (complex). The potential, Eq. (6) has been used successfully with the appropriate values of  $a$  and  $b$ . It has been found that when the TCS as a function of “ $b$ ” has a resonance [12], corresponding to the formation of a stable bound negative ion, this resonance is longest lived for a given value of the energy which corresponds to the electron affinity of the system (for ground state collisions) or the BE of the excited anion. This was found to be the case for all the systems we have investigated thus far. This fixes the optimal value of “ $b$ ” for Eq. (6).

In the calculation of the cross sections of the Tm, Lu and Hf atoms presented here, we have found three such values of  $b$  which still satisfy the TF equation within a reasonable error limit. We identify the three values with the resonance energies, corresponding to the formation of ground and excited negative ions of the atom under investigation. Note that the energies are measured relative to the ground-state of the neutral atom. The values used for “ $b$ ” in this paper are presented in Table 1 for the Tm, Lu and Hf

**Table 1**

Calculated binding energies, BE (eV), shape resonances, SR (eV), Ramsauer-Townsend (R-T) minima (eV) and  $b$  parameter for Tm, Lu and Hf atoms.

Z	Symbol	State	$b$	R-T	SR	BE
69	Tm	Ground	0.0342	0.074	0.212	0.274
		First excited	0.0452	–	0.035	0.108
		Second excited	0.0320	0.014	–	0.016
71	Lu	Ground	0.0365	0.076	0.239	0.415
		First excited	0.0479	–	0.037	0.104
		Second excited	0.0341	0.025	–	0.029
72	Hf	Ground	0.0377	0.076	0.266	0.525
		First excited	0.0493	–	0.0386	0.113
		Second excited	0.0350	0.015	–	0.017

atoms, while the value of “ $a$ ” was kept fixed at 0.2. The use in this paper of different values for the optimal parameter  $b$  for the ground and excited Tm, Lu and Hf atoms is supported by the recent study of low-energy electron scattering from Cu atoms [41]. There it was demonstrated that the ground and excited states are polarized differently as expected, namely both the dipole polarizability and quadrupole polarizability for the ground and the excited atomic Cu were found to be different.

For the numerical evaluation of the TCSs and the Mulholland partial cross sections, we solved the Schrödinger equation for complex values of  $L$  and real, positive values of  $E$

$$\Psi'' + 2\left(E - \frac{L(L+1)}{2r^2} - U(r)\right)\Psi = 0 \quad (7)$$

with the boundary conditions:

$$\begin{aligned} \Psi &= 0 \\ \Psi(r) &\sim e^{+i\sqrt{2E}r}, r \rightarrow \infty \end{aligned} \quad (8)$$

We note that Eq. (8) defines a bound state when  $k \equiv \sqrt{2E}$  is purely imaginary positive. In solving Eq. (8) two independent approaches were adopted. The first integrates numerically the radial Schrödinger equation for real integer  $\ell = \text{Re } L$  values of  $L$  to sufficiently large  $r$  values. The  $S$ -matrix is then obtained and the TCSs are evaluated as the traditional sum over partial waves, with the index of summation being  $\ell$ . The second part calculates the  $S$ -matrix,  $S(L, k)$  poles positions and residues of Eq. (7) following a method similar to that of Burke and Tate [42]. In the method the two linearly independent solutions,  $f_L$  and  $g_L$ , of the Schrödinger equation are evaluated as Bessel functions of complex order and the  $S$ -matrix, which is defined by the asymptotic boundary condition of the solution of the Schrödinger equation, is thus calculated. Further details of the calculation may be found in [42].

### 3. Results

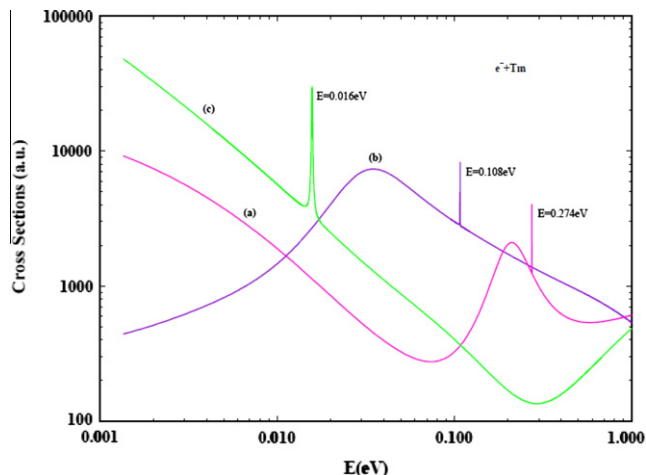
In the calculations we also need  $\text{Im } L$  which as mentioned above plays an important role. It is used to distinguish between the shape resonances (short-lived resonances) and the stable bound, both ground and excited, states of the negative ions (long-lived resonances) formed as Regge resonances in the electron–atom scattering [29,43]. In [43] and the applications [29] the physical interpretation of  $\text{Im } L$  is given. A small  $\text{Im } L$  implies that the system orbits many times before decaying, while a large  $\text{Im } L$  value denotes a short-lived state. For a true bound state, namely  $E < 0$ ,  $\text{Im } L \equiv 0$  so that the angular life,  $1/(\text{Im } L) \rightarrow \infty$ , implying that the system can never decay.  $\text{Im } L$  is also used to differentiate subtleties between the bound and the excited states of the negative ions formed as Regge resonances during the collisions. Generally,  $\text{Im } L$  for ground states is smaller than that for the excited states.

Experimental studies of the near-threshold electron attachment mechanism in neutral atoms, resulting in the formation of excited

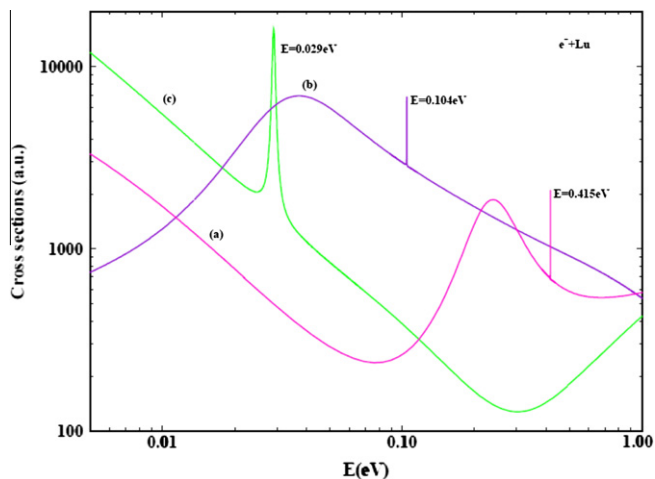
states of atomic negative ions that are bound with respect to the atomic ground state are very limited, and hardly exist theoretically. This has severely limited the knowledge of the existence and understanding of excited negative ions. Since the Regge-pole approach to low-energy electron attachment requires no prior knowledge of either experimental or other theoretical data, the Regge-pole methodology promises to enhance their exploration and advance their understanding.

Fig. 1 contrasts the electron elastic scattering TCSs for ground state, curve (a) and excited states, curves (b) and (c) for atomic Tm. Notably, the structure of each curve is significantly different from that of the other, demonstrating the importance of the core-polarization interaction. Curve (a) exhibits the typical characteristic behavior found in weakly bound systems [29], manifesting a Ramsauer-Townsend minimum at 0.0742 eV, a shape resonance at 0.212 eV and the stable bound ground Tm<sup>−</sup> anion at 0.274 eV formed during the collision as a Regge resonance. Curves (b) and (c) represent electron attachment resulting in excited Tm<sup>−</sup> negative ions; the binding energies of the first excited and second excited states are respectively 0.108 eV and 0.016 eV. The most important revelation in the comparisons is the appearance of the shape resonances between the bound state resonances of the negative ions. Both theoretical calculations and experimental measurements could easily mistake one for the other. This could also create problems in the use of the Wigner threshold law in high-precision measurements of BEs of valence electrons using photodetachment threshold spectroscopy. Furthermore, the determination of the R-T minimum could be problematic since it is together with the cross sections for the excited states.

In Fig. 2 is contrasted the electron elastic TCSs for Lu atoms. As in Fig. 1 curve (a) represents the data for the ground state Lu. This typical curve is characterized by a R-T minimum at 0.076 eV, a shape resonances at 0.239 eV and the BE of the Lu<sup>−</sup> anion at 0.415 eV formed during the collision as a resonance. Curve (b) represents the TCS for the first excited state, while curve (c) corresponds to that of the second excited state of the Lu atom. The BEs of the resultant excited negative ions formed during the collisions, are respectively 0.104 eV and 0.029 eV. As in Fig. 1 the shape resonances appear between the bound states of the Lu<sup>−</sup> negative ions. These shape resonances can be differentiated from the bound



**Fig. 1.** Total cross sections (a.u.) for electron elastic scattering from Tm atoms versus  $E$  (eV), are contrasted. Curves (a), (b) and (c) are respectively for the ground state, first excited state, and second excited state. All the curves are characterized by very sharp resonance structures corresponding to the binding energies of the resultant negative Tm<sup>−</sup> anions formed during the collisions. Curve (a) has the characteristic R-T minimum at 0.0742 eV, followed by a shape resonance at 0.212 eV and a stable bound ground state of the Tm<sup>−</sup> anion at 0.274 eV.



**Fig. 2.** The same as in Fig. 1, except that the data are for Lu atoms and the stable ground and excited bound states correspond to the  $\text{Lu}^-$  anions. The characteristic R-T minimum, the shape resonance and the stable bound ground state of the  $\text{Lu}^-$  anion are respectively at 0.076 eV, 0.239 eV and 0.415 eV.

states through the close scrutiny of the  $\text{Im } L$ , which for shape resonances is several orders-of-magnitude larger than that for the bound state resonances. As in Fig. 1, the presence of these resonances could be problematic in the application of the Wigner threshold law within the high precision measurements of BEs of valence electrons using photodetachment threshold spectroscopy.

Although the TCSs for the two atoms Tm and Lu appear to resemble one another, there are subtle differences. For example, the bound state of the  $\text{Lu}^-$  anion with the BE of 0.415 eV is closer to the nearby minimum as compared to that of the  $\text{Tm}^-$  anion with BE of 0.274 eV and is about a factor of two larger. Also the BE of the second excited state for the  $\text{Lu}^-$  anion is roughly a factor of two larger than that for the  $\text{Tm}^-$  anion. Interestingly, the ground state BEs and the second excited state BEs of the two atoms are affected significantly by their different electronic configurations, while the first excited state is insensitive to the differences in the electron configurations of the two atoms. The curves (c) of Figs. 1 and 2 do have R-T minima as well, which are at 0.014 eV and 0.025 eV, respectively. As pointed out in [33], the R-T minima are a manifestation of the polarization of the atomic core by the scattered electron. Their appearance signifies that the electron correlations are appropriately included in our Regge pole methodology.

Fig. 3 presents the results for the elastic scattering of an electron from Hf atoms. As in Figs. 1 and 2, the low-energy electron elastic scattering is characterized by three curves whose structures differ significantly from one another. For the Hf atom the results for the ground state with the EA of 0.525 eV and the second excited state curve with the BE of 0.017 eV have already been presented and discussed elsewhere [35]. The current exploration has revealed the presence of a first excited state of the  $\text{Hf}^-$  anion at 0.113 eV (represented by the green curve). We note that this value is very close to that calculated by Pan and Beck [14] and claimed to correspond to the EA of the Hf atom. The identification is certainly incorrect since the EA of Hf is 0.525 eV.

As seen from the figure it is difficult to identify the various resonances without actually plotting the TCSs and utilizing  $\text{Im } L$  since the bound state resonances (both ground and excited states) and the shape resonances are all mixed together. The importance and utility of the present investigation are clearly demonstrated. It is also noted that the ground state TCS is characterized by a deep R-T minimum followed by a shape resonance, the bound state of the stable  $\text{Hf}^-$  negative ion and a shallow minimum. The parameters of the various curves are presented in Table 1, where they are compared with those of the Tm and the Lu atoms.

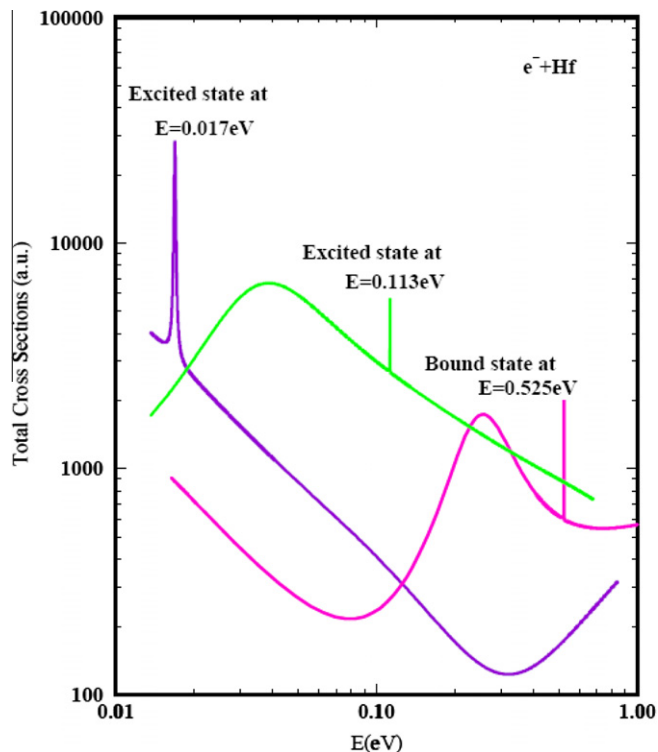


**Fig. 3.** The same as in Fig. 1, except that the data are for Hf atoms and the stable ground and excited bound states correspond to the  $\text{Hf}^-$  anions. The characteristic R-T minimum, the shape resonance and the stable bound ground state of the  $\text{Hf}^-$  anion are respectively at 0.076 eV, 0.266 eV and 0.525 eV.

The DCSs provide a stringent test of theoretical calculations when the results are compared with those of reliable measurements; therefore they will be useful in this context in the future. Panels (a–c) of Fig. 4 present the DCSs (a.u.) in energy at  $\theta = 0^\circ$ ,  $90^\circ$  and  $180^\circ$  for the electron elastic collisions, resulting in the formation of ground, first excited and second excited  $\text{Tm}^-$  anions, respectively. Most significant about these curves is that the DCSs are also characterized by dramatically sharp peaks at  $\theta = 0^\circ$ ,  $90^\circ$  and  $180^\circ$ , corresponding to the values of the BEs, viz. 0.274 eV, 0.108 eV and 0.016 eV, respectively of the stable bound  $\text{Tm}^-$  anions, formed during the collision as resonances. The DCSs at  $\theta = 180^\circ$  also yield the BEs, but the peaks have become mainly anti-resonances (see Fig. 4, panels (a) and (b)). Preceding the stable bound states of the  $\text{Tm}^-$  anions in panels (a) and (b) are the broader peaks that correspond to the shape resonances as described above under the TCSs. The DCSs critical minima [44,45] are identifiable at 0.102 eV and 0.20 eV in panels (a) and (c), respectively. A critical minimum does exist in the DCSs of panel (b) but it is at a higher energy value than the figure could accommodate. Clearly, the DCSs are quite different from one another in the three panels, reflecting the dynamical processes taking place at the various ground and excited states levels. For example, in the figures the DCSs at  $\theta = 0^\circ$  and  $90^\circ$  capture the essentials of the TCSs of Fig. 1. Additionally, the critical minima appear at different positions relative to the bound states of the  $\text{Tm}^-$  negative ion.

The panels (a–c) of Fig. 5 present the DCSs (a.u.) in energy at  $\theta = 0^\circ$ ,  $90^\circ$  and  $180^\circ$  for the electron elastic collisions, resulting in the formation of ground, first excited and second excited  $\text{Tm}^-$  anions, respectively. Except for minor details, the results are essentially the same as those of Fig. 4, including the description. So, we will not repeat their description here. However, it is worth pointing out that the values of the BEs are different; they are 0.415 eV, 0.104 eV and 0.029 eV for the ground, first excited and second excited states, respectively for the  $\text{Lu}^-$  negative ions formed

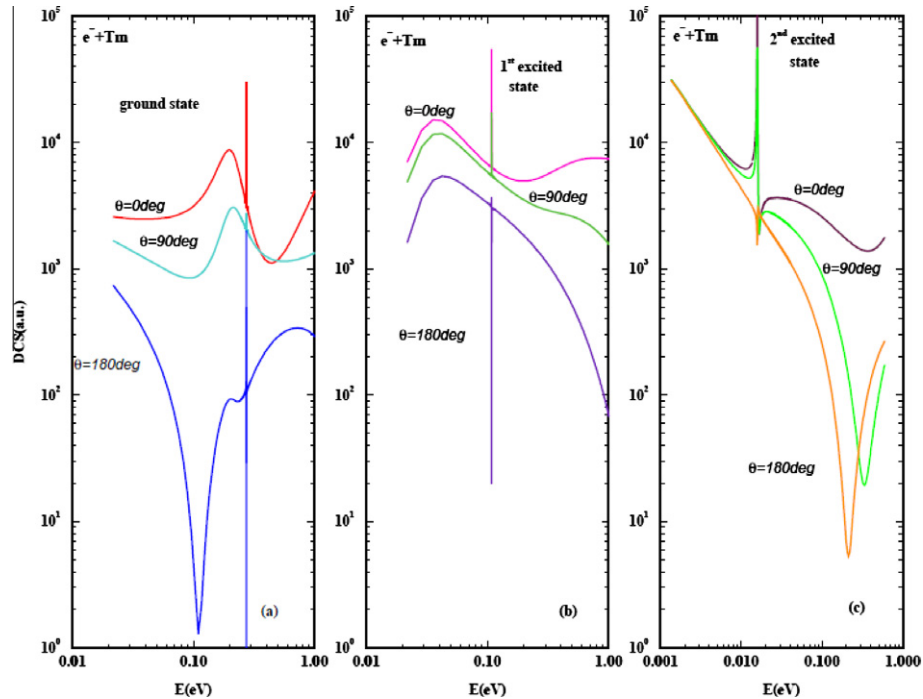


**Fig. 4.** Differential cross sections for electron elastic scattering from Tm versus  $E$  (eV) at the scattering angles  $\theta = 0^\circ, 90^\circ$  and  $180^\circ$ . Panels (a), (b) and (c) are respectively for the ground state, first excited state, and second excited state. All the curves in the panels are characterized by very sharp resonance structures corresponding to the binding energies of the resultant  $\text{Tm}^-$  negative ions formed during the collisions.

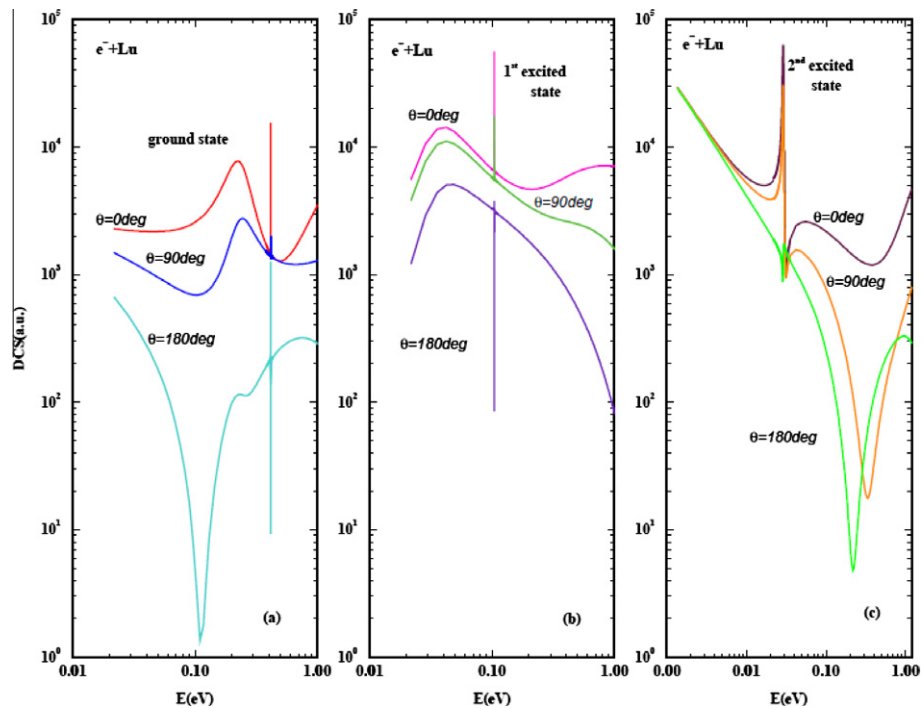


**Fig. 5.** The same as in Fig. 4, except that the data are for Lu atoms and the stable ground and excited bound states correspond to the  $\text{Lu}^-$  anions. All the curves in the panels are characterized by very sharp resonance structures corresponding to the binding energies of the resultant  $\text{Lu}^-$  negative ions formed during the collisions.

during the collision as resonances. Here the DCSs critical minima [44,45] are also identifiable at 0.102 eV and 0.22 eV in panels (a) and (c), respectively. For Fig. 5(b) the DCS critical minimum is at a higher energy value than could be accommodated by the figure.

In Fig. 6 the panels (a–c) present the DCSs (a.u.) in energy at  $\theta = 0^\circ, 90^\circ$  and  $180^\circ$  for the electron–Hf elastic collision, resulting in the formation of ground, first excited and second excited Hf<sup>−</sup>

anions, respectively. Except for minor details, the DCSs are essentially the same as those of Figs. 4 and 5. So, we will not repeat their description here. However, the BEs are quite different; they are 0.525 eV, 0.113 eV and 0.017 eV for the ground, first excited and second excited states, respectively for the Hf<sup>−</sup> negative ions formed during the collision as resonances. Here the DCSs critical minima [44,45] are also identifiable at 0.102 eV and 0.22 eV in panels (a)

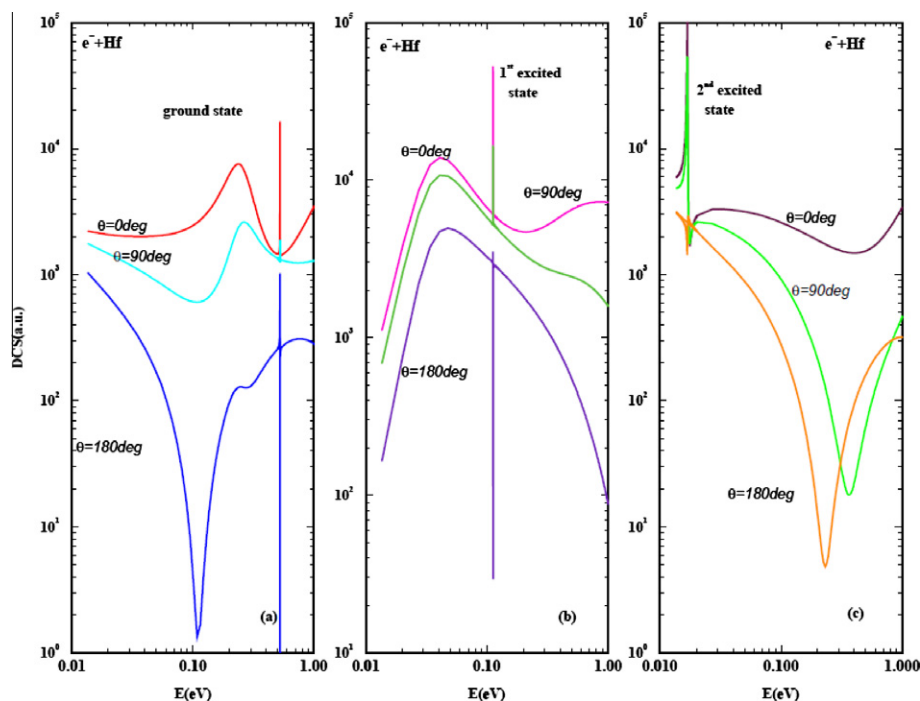


**Fig. 6.** The same as in Fig. 4, except that the data are for Hf atoms and the stable ground and excited bound states correspond to the  $\text{Hf}^-$  anions. All the curves in the panels are characterized by very sharp resonance structures corresponding to the binding energies of the resultant  $\text{Hf}^-$  negative ions formed during the collisions.

and (c), respectively. Interestingly, the DCS critical minima in Hf maintain the same positions as in Tm and Lu.

Just as mentioned previously in the cases of gold and platinum atoms [46], it might be easier for experiments to search for the predicted excited negative ions of  $\text{Tm}^-$ ,  $\text{Lu}^-$  and  $\text{Hf}^-$  through the investigation of the DCSs in energy at  $\theta = 0^\circ$ ,  $90^\circ$  and  $180^\circ$  as well as in scattering angles. Clearly, complications in the resonance structure arising from the superposition of the structures from the ground and excited states could easily lead to the wrong identification and interpretation. Also, this could interfere with the use of the Wigner threshold law through the presence of many resonances. Hence, the need for the identification and delineation of the near-threshold resonance structures in low energy electron scattering from neutral atoms.

Table 1 summarizes the results of the calculations for Tm, Lu and Hf atoms. We note that the BE value of 0.113 eV for  $\text{Hf}^-$  is very close to the recent value of 0.114 eV identified with the EA of Hf by [14]. Clearly, this value cannot correspond to the EA since it is not the lowest.

#### 4. Summary and conclusions

Low-energy  $E \leq 1.0$  eV electron elastic scattering from the Tm, Lu and Hf complex atoms has been investigated, searching for electron attachment manifesting as Regge resonances in the TCSs. We found that the electron collision TCSs and the DCSs for these atoms are characterized by dramatically sharp resonances, corresponding to the formation of stable negative ions. From the energy positions of the resonances we have extracted the BEs of the ground, first and second excited states of the  $\text{Tm}^-$ ,  $\text{Lu}^-$  and  $\text{Hf}^-$  negative ions formed during the collisions. The imaginary part of the complex angular momentum has been used to differentiate between the shape resonances and the stable bound states of the negative ions. Shape resonances and R-T minima have been identified and delineated in the TCSs, including the attendant critical minima of the DCSs. Clearly, the DCSs provide a new powerful approach to the investigation of low energy electron attachment to atoms,

resulting in the formation of stable ground and excited negative ions as resonances. The cross sections for both the ground and excited Tm, Lu and Hf atoms obtained here call for experimental verification.

This first theoretical prediction of two excited negative ionic states in atoms is expected to enhance significantly the interpretation of electron-induced chemical processes resulting in negative ion formation. It proclaims new frontiers of efficient design and synthesis of novel functional compounds and catalysts for various chemical reactions, impacting many industries and technologies. Indeed, the identification and delineation of the resonance structures and minima in the electron collision TCSs for atoms in the near threshold energy region is also toward the realization of the proposed spectroscopy of slow electrons [47]. The spectroscopy is realized through the observation of the formation of tenuously bound,  $\text{BE} \leq 0.1$  eV and weakly bound,  $\text{BE} < 1$  eV negative ionic states for the detection of nanomaterials.

#### Acknowledgments

Research was supported by the US DOE, Division of Chemical Sciences, Office of Basic Energy Sciences, Office of Energy Research and the AFOSR Grant No. FA9550-09-1-0672. This research used resources of the National Energy Research Scientific Computing Center, which is supported by the Office of Science of the US DOE under Contract No. DE-AC02-05CH11231. DS is supported by IKER-BASQUE, Basque Foundation for Science. The computing facilities of the Queen's University of Belfast, UK are also greatly appreciated.

#### References

- [1] A.Z. Msezane, Z. Felfli, D. Sokolovski, J. Phys. B 43 (2010) 201001 (FAST TRACT).
- [2] J.K. Edwards, A.F. Carley, A.A. Herzing, C.J. Kiely, G.J. Hutchings, J. Chem. Soc., Faraday Discuss. 138 (2008) 225.
- [3] J.K. Edwards, B. Solsona, P. Landon, A.F. Carley, A. Herzing, M. Watanabe, C.J. Kiely, G.J. Hutchings, J. Mater. Chem. 15 (2005) 4595.
- [4] M.S. Wong, P.J.J. Alvarez, Y.L. Fang, N. Akcin, M.O. Nutt, J.T. Miller, K.N. Heck, J. Chem. Technol. Biotechnol. 84 (2009) 158.

- [5] V.I. Lengyel, V.T. Navrotsky, E.P. Sabad, *Resonance Phenomena in Electron-Atom Collisions*, Springer-Verlag, Berlin, 1992 (Chapter 7).
- [6] A. Jones, P. Caradonna, C. Makochekanwa, D. Slaughter, D. Mueller, J.P. Sullivan, S.J. Buckman, *J. Phys.: Conf. Ser.* 194 (2009) 012033.
- [7] V.V. Petrunin, M. Harbst, T. Andersen, *Phys. Rev. A* 63 (2001) 030701.
- [8] M. Scheer, R.C. Bilodeau, C.A. Brodie, H.K. Haugen, *Phys. Rev. A* 58 (1998) 2844.
- [9] T.M. Miller, A.E. Stevens Miller, W.C. Lineberger, *Phys. Rev. A* 33 (1986) 3558.
- [10] J. Thogersen, L.D. Steele, M. Scheer, C.A. Brodie, H.K. Haugen, *J. Phys. B* 29 (1996) 1323.
- [11] A.M. Covington, D. Calabrese, J.S. Thompson, T.J. Kvale, *J. Phys. B* 31 (1998) L855.
- [12] D. Sokolovski, Z. Felfli, S.Y. Ovchinnikov, J.H. Macek, A.Z. Msezane, *Phys. Rev. A* 76 (2007) 012705.
- [13] P. Andersson, A.O. Lindahl, D. Hanstorp, D.J. Pegg, *Phys. Rev. A* 79 (2009) 022502.
- [14] L. Pan, D.R. Beck, *J. Phys. B* 43 (2010) 025002.
- [15] P. Andersson, A.O. Lindahl, C. Alfredsson, L. Rogstrom, C. Diehl, D.J. Pegg, D. Hanstorp, *J. Phys. B* 40 (2007) 4097.
- [16] M.H.F. Bettega, C. Winstead, V. McKoy, *Phys. Rev. A* 74 (2006) 022711.
- [17] V.V. Petrunin, H.H. Andersen, P. Balling, T. Andersen, *Phys. Rev. Lett.* 76 (1996) 744.
- [18] J. Wu, J. Yuan, *J. Phys. B* 39 (2006) 2493.
- [19] H.W. van der Hart, C. Laughlin, J.E. Hansen, *Phys. Rev. Lett.* 71 (1993) 1506.
- [20] V.V. Petrunin, J.D. Voldstad, P. Balling, P. Kristensen, T. Andersen, H.K. Haugen, *Phys. Rev. Lett.* 75 (1995) 1911.
- [21] K.L. Baluja, A.Z. Msezane, *J. Phys. B* 34 (2001) 3157.
- [22] T. Stoecklin, F.A. Gianturco, *Eur. Phys. J. D* 40 (2006) 369.
- [23] D.R. Bates, *Adv. Atom. Mol. Opt. Phys.* 27 (1991) 1; C. Blondel, *Phys. Scr. T* 58 (1995) 31.
- [24] T. Andersen, *Phys. Rep.* 394 (2004) 157.
- [25] D.J. Pegg, *Rep. Prog. Phys.* 67 (2004) 857.
- [26] S.J. Buckman, C.W. Clark, *Rev. Mod. Phys.* 66 (1994) 539.
- [27] S.A. Napier, D. Cvejanovic, P.D. Burrow, J.F. Williams, J.A. Michejda, L. Pravica, *Phys. Rev. A* 80 (2009) 042710.
- [28] A.Z. Msezane, Z. Felfli, D. Sokolovski, *Chem. Phys. Lett.* 456 (2008) 96.
- [29] Z. Felfli, A.Z. Msezane, D. Sokolovski, *Phys. Rev. A* 79 (2009) 012714.
- [30] H. Hotop, M.-W. Ruf, I.I. Fabrikant, *Phys. Scr. T* 110 (2004) 22.
- [31] E.P. Wigner, *Phys. Rev.* 73 (1948) 1002.
- [32] T. Andersen, H.K. Haugen, H. Hotop, *J. Phys. Chem. Ref. Data* 28 (1999) 1511.
- [33] W.R. Johnson, C. Guet, *Phys. Rev. A* 49 (1994) 1041.
- [34] S. Aubin, S. Myrskog, M.H.T. Extavour, L.J. LeBlanc, D. McKay, A. Stummer, J.H. Thywissen, *Nat. Phys.* 2 (2006) 384.
- [35] Z. Felfli, A.Z. Msezane, D. Sokolovski, *Phys. Rev. A* 81 (2010) 042707.
- [36] J.H. Macek, P.S. Krstic, S.Yu. Ovchinnikov, *Phys. Rev. Lett.* 93 (2004) 183203.
- [37] H.P. Mulholland, *Proc. Cambridge Philos. Soc. (London)* 24 (1928) 280.
- [38] L.H. Thomas, *Philos. Soc.* 23 (1924) 542; E. Fermi, *Zeit. Phys.* 48 (1928) 73.
- [39] S. Belov, N.B. Avdonina, Z. Felfli, M. Marletta, A.Z. Msezane, S.N. Naboko, *J. Phys. A* 37 (2004) 6943.
- [40] S. Belov, K.-E. Thylwe, M. Marletta, A.Z. Msezane, S. Naboko, *J. Phys. A* 43 (2010) 365301.
- [41] S.Y. Yousif Al-Mulla, *Eur. Phys. J. D* 42 (2007) 11.
- [42] P.G. Burke, C. Tate, *Comp. Phys. Commun.* 1 (1969) 97.
- [43] J.N.L. Connor, *J. Chem. Soc., Faraday Trans.* 86 (1990) 1627.
- [44] A.R. Milosavljevic, D. Sevic, B.P. Marinkovic, *J. Phys. B* 37 (2004) 4681.
- [45] J.E. Sienkiewicz, S. Telega, P. Syty, S. Fritzsche, *Phys. Lett. A* 293 (2002) 183.
- [46] Z. Felfli, A.R. Eure, A.Z. Msezane, D. Sokolovski, *Nucl. Instrum. Methods Phys. Res. B* 268 (2010) 1370.
- [47] A.Z. Msezane, Z. Felfli, D. Sokolovski, arXiv:arXiv:0901.1124v1.